DOI: 10.1002/adsc.201600498

Advanced Synthesis & Catalysis

1,3-Diamine-Derived Bifunctional Organocatalyst Prepared from Camphor

Sebastijan Ričko,[a] Jurij Svete,[a] Bogdan Štefane,[a] Andrej Perdih,[b] Amalija Golobič,[a] Anže Meden,[a] and Uroš Grošelj[a,*]

[a] Faculty of Chemistry and Chemical Technology, University of Ljubljana, Večna pot 113, SI-1000 Ljubljana, Slovenia
Fax: (+386)-1-2419-144; phone: (+386)-1-479-8563; e-mail: uros.groselj@fkkt.uni-lj.si
[b] National Institute of Chemistry, Hajdrihova 19, SI-1000 Ljubljana, Slovenia

Received: May 11, 2016; Revised: September 13, 2016; Published online: ■■ ▮▮, 0000

Dedicated to Professor Emeritus Miha Tišler, University of Ljubljana, on the occasion of his 90th birthday.

Supporting information for this article is available on the WWW under http://dx.doi.org/10.1002/adsc.201600498.

Abstract: Chiral 1,2-diamines are privileged structural motifs in organocatalysis, whereas efficient 1,3-diamine-derived organocatalysts are very rare. Herein we report a highly efficient camphor-1,3-diamine-derived squaramide organocatalyst. Its catalytic activity in Michael additions of 1,3-dicarbonyl nucleophiles to *trans*-β-nitrostyrene derivatives provides excellent enantioselectivities (up to >99% *ee*).

Keywords: camphor; 1,3-diamines; Michael addition; organocatalysis; squaramides

Introduction

Inspired by the efficiency and selectivity of enzymatic catalysis, the design of organic molecules capable of catalyzing efficient and stereoselective C–C bond formation is a formidable challenge, which is nowadays receiving considerable attention.[1] One of the fundamental enzymatic catalyst competences that is difficult to mimic in synthetic systems is bifunctionality; that is, the ability of a catalyst possessing acid and base functionality to synergistically activate both the nucleophile and the electrophile reacting partners, simultaneously.[2–4] The advent of organocatalysis in the last decades has provided a boost to the development of organocatalyzed synthetic processes for the stereoselective formation of C–C and C–X bonds including the construction of useful complex organic frameworks.[5]

The possibility to sterically and/or electronically modulate the structure of chiral 1,2-diamines has rendered them privileged structural motifs in organic synthesis. They are indispensable in stereoselective catalysis ranging from transition metal-catalyzed reactions[6,7] to organocatalysis.[2–4,7] Since the pioneering work of Jacobsen,[8] Schreiner,[9] and Takemoto,[10] bifunctional amine-thioureas have become one of the most versatile catalyst types in asymmetric organocatalysis.[2,3] The scope of bifunctional organocatalysis has then been expanded by replacing the thiourea with a squaramide moiety.[2,4] Consequently, amine-thiourea and amine-squaramide catalysts have become work horses of non-covalent organocatalysis. In spite of their tremendous utility, these organocatalysts are derived from a limited range of chiral structural scaffolds with the 1,2-diamine moiety as a common structural motif.[2–4,11] In contrast, efficient 1,3- and 1,4-diamine-derived organocatalysts [with the exception of (BINAM)-based catalysts] are very rare. Conformationally flexible guanidine-bisthiourea organocatalysts have been used in asymmetric 1,4-type Friedel–Crafts reaction of phenols[12a] and phospha-Michael reaction of diphenyl phosphonate with nitroolefins.[12b] Ferrocene-based[12c,d] and self-assembled proline-1,3-diamine-thiourea[12e] bifunctional organocatalysts showed high enantioselectivity in Michael additions of acetylacetone and aldehydes to nitroolefins. On the other hand, tartaric acid-based 1,4-diamine-thiourea organocatalysts were not effective in the above additions (Figure 1).[12f]

Camphor is one of nature's privileged scaffolds readily available in both enantiomeric forms. It undergoes a wide variety of chemical transformations which functionalize, at first glance, inactivated positions, thus enabling the preparation of structurally and functionally very diverse products. All of the above features make camphor a highly desirable starting mate-

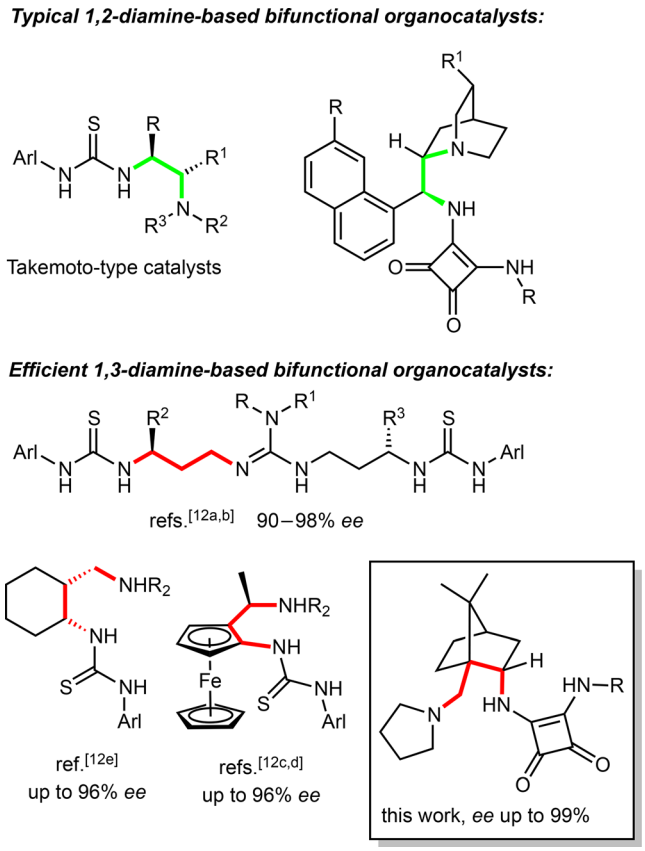

Figure 1. Examples of typical 1,2-diamine-thiourea organocatalysts and efficient 1,3-diamine analogues.

rial.[13] The first reports on the application of camphor-derived organocatalysts date back to 2005,[14] while this topic has recently also been reviewed.[15] Structurally, these organocatalysts are divided into two categories. The first, minor one, comprises catalysts with a camphor skeleton as the exclusive chiral framework with camphor-derived NHC precursors and cyclic hydrazides as typical representatives.[14a,15,16] The vast majority of camphor-based organocatalysts constitute the second category of mixed bifunctional organocatalysts, where the camphor framework is covalently connected through a suitable spacer to an α-amino acid, most frequently a proline derivative.[15,17]

Within our continuing study on camphor-based diamines as potential organocatalyst scaffolds,[18] we herein report the synthesis of a novel type of 1,3-diamine-derived bifunctional squaramide organocatalysts prepared from camphor and their application as highly efficient catalysts in Michael additions of 1,3-dicarbonyl nucleophiles to *trans*-β-nitrostyrenes.

Results and Discussion

First, non-racemic 1,3-diamines **4** and **5** were prepared in four steps from (1*S*)-(+)-10-camphorsulfonic acid. Following a literature procedure, camphorsulfonic acid was transformed into 10-iodocamphor (**1**),[19] which was further converted with pyrrolidine into the amino ketone **2**. To the best of our knowledge, the above transformation represents the easiest way to prepare 10-aminocamphor derivatives. Subsequent condensation of **2** with NH_2OH, and reduction of the so-formed oxime **3** yielded a chromatographically separable mixture of the minor *exo*- **4** and the major *endo*-1,3-diamine **5** in moderate overall yields (Scheme 1).

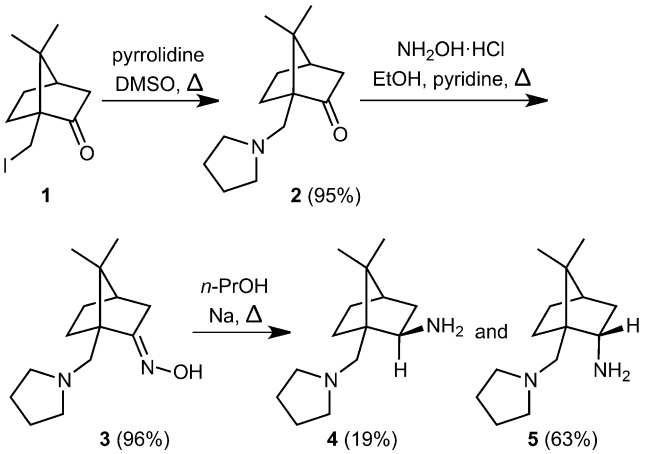

Scheme 1. Synthesis of camphor-derived 1,3-diamines **4** and **5**.

Next, the title organocatalysts **8**–**12** were prepared in 26–84% yields by condensation of diamines **4** and **5** with squaramates **6a**–**c**[4e,20] or squarate **7**. To have access to racemic products for HPLC analysis, a new achiral organocatalyst **13** was also prepared from squaramate **6a** and *N*,*N*-dimethylethylenediamine (**14**) (Scheme 2). The structures of organocatalysts **9** and **10** were confirmed by single crystal X-ray analysis (Figure 2).[21,22]

Initially, organocatalysts **8**–**12** (5 mol% used) were tested in the 1,4-addition reaction of acetylacetone (**15**) to *trans*-β-nitrostyrene (**16a**) in toluene at 25 °C for 24 h. The results are presented in Table 1. Compound **9** was quickly established as the superior organocatalyst, both in terms of conversion (>99%) and enantioselectivity (>98% *ee*) (entries 1–5). Screening of the above reaction in various solvents (catalyst **9**, 25 °C, 24 h, entries 6–16) revealed that reactions generally proceeded with excellent conversions (≥97%) and enantioselectivities (≥95% *ee*), though the conversion was slower in 1,4-dioxane and MeCN (entries 6 and 14). Diminished enantioselectivities were observed in MeCN (90% *ee*) and MeOH (79% *ee*) (entries 14 and 13). Reaction in brine gave **17a** in 96% *ee* (entry 15), while the neat reaction gave **17a** in 93% *ee* (entry 16).

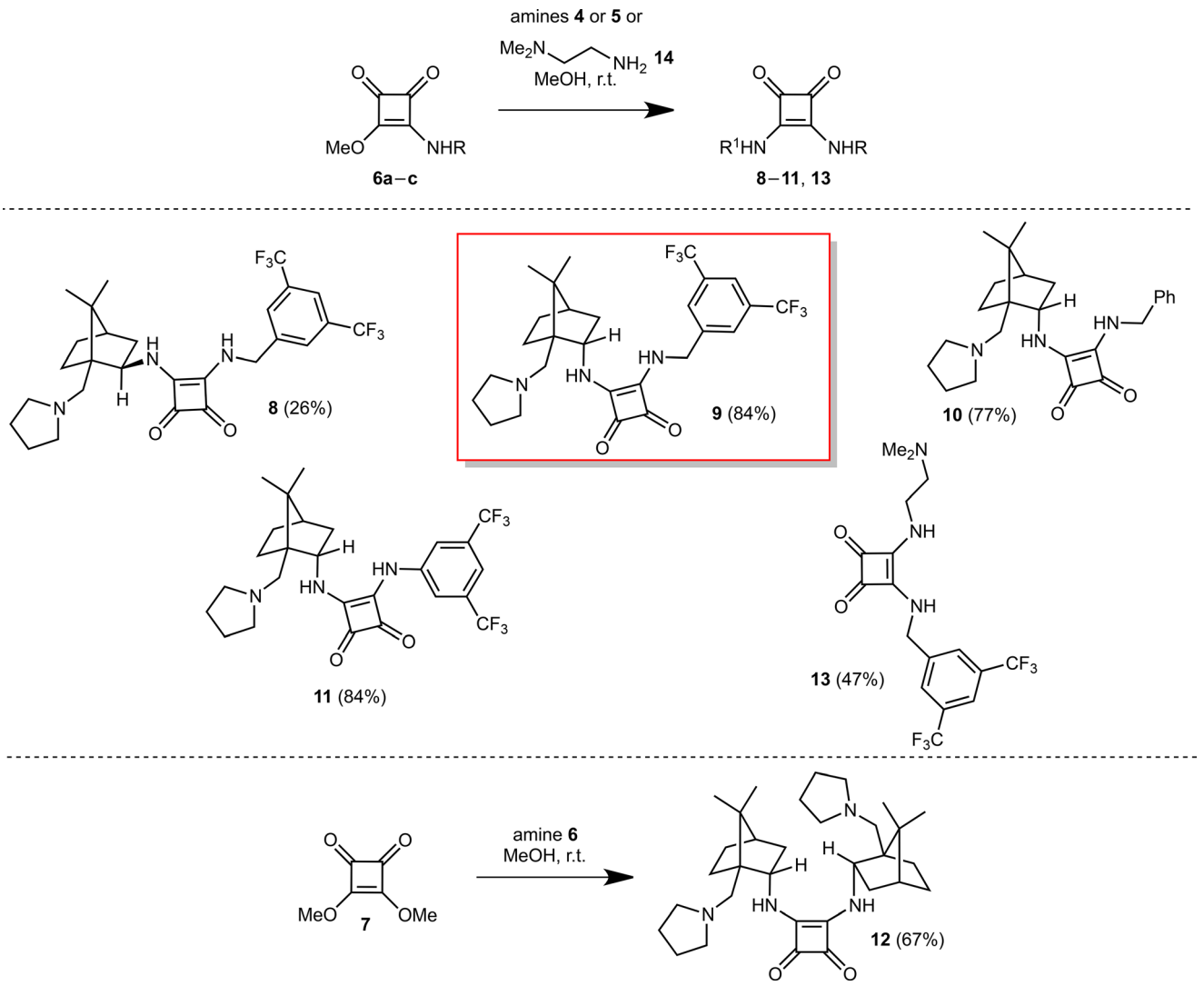

Scheme 2. Synthesis of squaramide organocatalysts **8**–**13**.

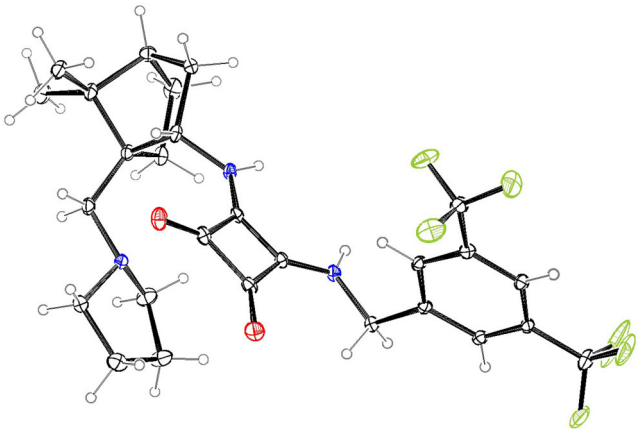

Figure 2. ORTEP representation of single-crystal X-ray structure of compound **9**. Ellipsoids are plotted at 30% probability level.[21,22]

Toluene was chosen as the solvent to be used in further transformations. Reactions at lower temperature (0 °C and −25 °C) were even more enantioselective (>99% *ee*), albeit with slower conversion (entries 17 and 18). The conversion was much faster at 80 °C, with only slight decrease of enantioselectivity (entry 19). Lowering the catalyst loading to 0.1 mol% slowed down the conversion substantially, while enantioselectivity was only slightly decreased (entry 20).[21] Under the optimum reaction conditions (toluene, 25 °C, 24 h), the Rawal's squaramide catalyst **I**,[4e] Takemoto's thiourea catalyst **II**,[10a] and Rawal-type cyclohexane-1,2-diamine-based squaramide catalyst **III**[5f] were all outperformed by the catalyst **9** (entries 21–23 *vs.* entry 2). Notably, the efficacy of catalysts **I**–**III**[21] under the above conditions was also in line with the literature data.[4e,10a,5f]

Catalyst **9** was then evaluated in the alkylation of acetylacetone (**15**) with *trans*-β-nitrostyrenes **16b**–

Table 1. Evaluation and optimization of organocatalysts **8**–**12** in the Michael addition of acetylacetone (**15**) to *trans*-β-nitrostyrene (**16a**).[a]

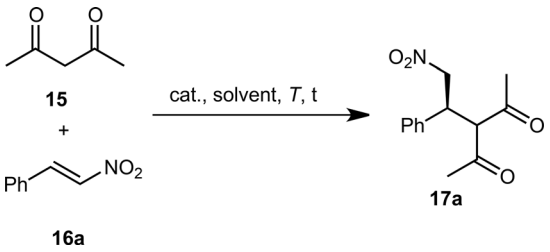

Entry	Cat. (mol%)	Solvent	*t* [h]/ *T* [°C]	Conv. [%]	*ee* [%]
1	**8** (5)	toluene	24/25	84	34 (*R*)
2	**9** (5)	toluene	24/25	>99 (85)[b]	98 (*S*)
3	**10** (5)	toluene	24/25	53	96 (*S*)
4	**11** (5)	toluene	24/25	40	90 (*S*)
5	**12** (5)	toluene	24/25	81	82 (*S*)
6	**9** (5)	1,4-dioxane	24/25	57	97 (*S*)
7	**9** (5)	$CHCl_3$	24/25	>99	96 (*S*)
8	**9** (5)	EtOAc	24/25	97	96 (*S*)
9	**9** (5)	THF	24/25	98	98 (*S*)
10	**9** (5)	CH_2Cl_2	24/25	>99	95 (*S*)
11	**9** (5)	$PhCF_3$	24/25	>99	98 (*S*)
12	**9** (5)	AcAc	24/25	>99	96 (*S*)
13	**9** (5)	MeOH	24/25	>99	79 (*S*)
14	**9** (5)	MeCN	24/25	60	90 (*S*)
15	**9** (5)	brine	24/25	>99	96 (*S*)
16	**9** (5)	neat	24/25	>99	93 (*S*)
17	**9** (5)	toluene	24/0	76	>99 (*S*)
18	**9** (5)	toluene	24/−25	43	>99 (*S*)
19	**9** (5)	toluene	3/80	96	94 (*S*)
20	**9** (0.1)	toluene	24/80	31	93 (*S*)
21	**I**[c] (5)	toluene	24/25	98	96 (*R*)
22	**II**[c] (5)	toluene	24	>99	88 (*R*)
23	**III**[c] (5)	toluene	24/25	>99	88 (*R*)

[a] Acetylacetone (**15**) (0.8 mmol), *trans*-β-nitrostyrene (**16a**) (0.4 mmol), solvent (1.0 mL); conversion determined by ^{1}H NMR ($CDCl_3$); *ee* determined by HPLC.[21]
[b] Isolated yield.
[c] **I** = Rawal's squaramide catalyst;[4e] **II** = Takemoto's thiourea catalyst;[10a] **III** = Rawal-type cyclohexane-1,2-diamine-squaramide catalyst;[5f] the structures of **I**–**III** are given in the Supporting Information.

Table 2. Variation of nitroalkene **16b–s** in reactions with acetylacetone (**15**).[a]

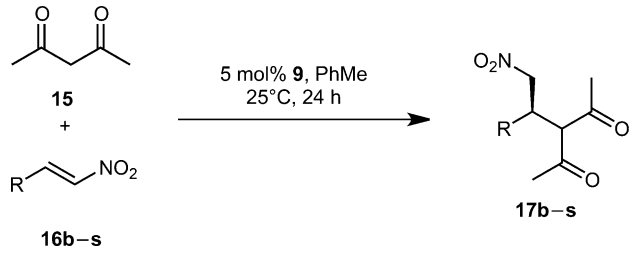

Entry	R	Product	Yield [%][b]	*ee* [%]
1	4-MeO-C_6H_4 (**16b**)	**17b**	86 (91)	99
2	3-MeO-C_6H_4 (**16c**)	**17c**	85 (>99)	98
3	2-MeO-C_6H_4 (**16d**)	**17d**	89 (92)	>99
4	2,5-MeO-C_6H_3 (**16e**)	**17e**	86 (>99)	98
5	4-BnO-C_6H_4 (**16f**)	**17f**	62 (73)	92
6	2-BnO-C_6H_4 (**16g**)	**17g**	92 (>99)	>99
7	3,4-BnO-C_6H_3 (**16h**)	**17h**	72 (80)	99
8	2-F-C_6H_4 (**16i**)	**17i**	81 (>99)	99
9	4-Cl-C_6H_4 (**16j**)	**17j**	79 (>99)	>99
10	3-Cl-C_6H_4 (**16k**)	**17k**	68 (>99)	96
11	2-Cl-C_6H_4 (**16l**)	**17l**	76 (>99)	>99
12	2,4-Cl-C_6H_3 (**16m**)	**17m**	73 (>99)	>99
13	2,6-Cl-C_6H_3 (**16n**)	**17n**	63 (82)	91
14	3-Br-C_6H_4 (**16o**)	**17o**	80 (>99)	94
15	2-Br-C_6H_4 (**16p**)	**17p**	87 (>99)	>99
16	2-furyl (**16q**)	**17q**	54 (97)	98
17	1-propyl (**16r**)	**17r**	43 (72)	>99
18	2-propyl (**16s**)	**17s**	9 (17)	86

[a] Acetylacetone (**15**) (0.8 mmol), nitroalkene **16b–s** (0.4 mmol), toluene (1.0 mL); conversion determined by ^{1}H NMR ($CDCl_3$); *ee* determined by HPLC.[21]
[b] Isolated yields; the conversions are given in the brackets.

s under the optimum reaction conditions (toluene, 25 °C, 24 h). The results are presented in Table 2. Generally, the conversions were quantitative (≥97%). A moderate slowdown was observed in the case of electron-donating substituents (entries 1, 3, 5, and 7) and two *ortho*-substituents (entry 13). Enantioselectivities were high (>90% *ee*), in most cases even excellent (>98% *ee*). Notably, persistently high selectivities were obtained using *ortho*-monosubstituted nitrostyrenes (entries 3, 4, 6, 8, 11, 12, and 15). In the reactions of **15** with aliphatic 1-nitroalkenes **16r** and **16s**, the enantioselectivities were essentially the same as in the β-nitrostyrene series **16a–q**, while the yields were lower (entries 17 and 18).

To further explore the scope of the studied catalytic system, catalyst **9** was evaluated in 1,4-addition reactions of nitrostyrenes **16a**, **16i**, **16l**, and **16p** with selected 1,3-diketones and β-keto esters **18a–h** (Table 3). Once again, almost all reactions proceeded with excellent conversion, while diastereoselectivity varied with the nucleophile applied; in most cases mixtures of diastereomers were formed. Excellent diastereoselectivity (*dr* > 94:6) was observed in reactions with ethyl 2-oxocyclopentane-1-carboxylate (**18f**) and its 6-membered analogue **18h** (entries 9 and 13), and in the reaction between α-acetylbutyrolactone (**18g**) and *trans*-2-bromo-β-nitrostyrene (**16p**) (entry 12). The *ee* of the products ranged from 73% to >99%, most of them being ≥96% *ee*. Also here, the presence of an *ortho*-substituent in nitrostyrenes **16i**, **16l**, and **16p** increased the enantioselectivity in comparison to reactions with *ortho*-unsubstituted ni-

Table 3. Variation of nucleophile **18a–h** in reactions with nitrostyrenes **16a**, **i**, **l**, **p**.[a]

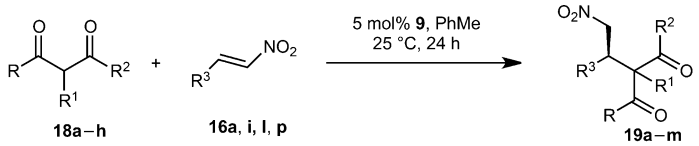

18a–h **16a, i, l, p** **19a–m**

Entry	Nucleophile	Nitroalkene	Product		Yield [%][b]	*dr*	*ee* [%]
1	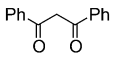 **18a**	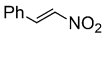 **16a**	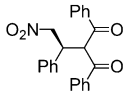	**19a**	34 (40)	-	97
2	 **18b**	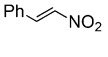 **16a**	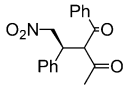	**19b**	84 (>99)	72:28	98, 97
3	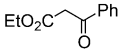 **18c**	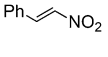 **16a**	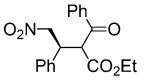	**19c**	69 (>99)	78:22	96, 76
4	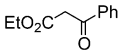 **18c**	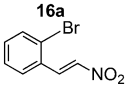 **16p**	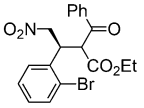	**19d**	86 (>99)	53:47	98, 98
5	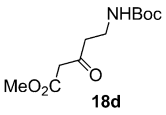 **18d**	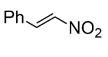 **16a**	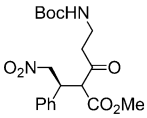	**19e**	95 (>99)	51:49	98, >99
6	 **18e**	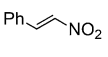 **16a**	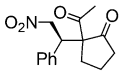	**19f**	91 (>99)	76:24	98, 91
7	 **18e**	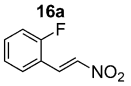 **16i**	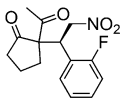	**19g**	83 (94)	68:32	99, 97
8	 **18e**	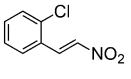 **16l**	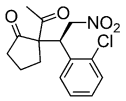	**19h**	89 (96)	53:47	97, >99
9	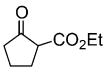 **18f**	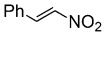 **16a**	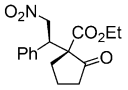	**19i**	94 (>99)	97:3	98, -
10	 **18g**	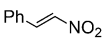 **16a**	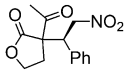	**19j**	85 (>99)	67:33	73, 89
11	 **18g**	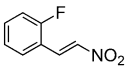 **16i**	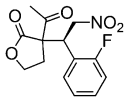	**19k**	77 (>99)	74:26	92, 94
12	 **18g**	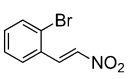 **16p**	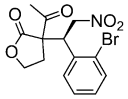	**19l**	85 (>99)	94:6	99, -
13	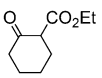 **18h**	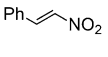 **16a**	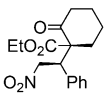	**19m**	39 (47)	99:1	>99, -

[a] Nucleophile (0.8 mmol), nitrostyrene (0.4 mmol), toluene (1.0 mL); conversion and *dr* determined by ^{1}H NMR ($CDCl_3$); *ee* determined by HPLC.[21]

[b] Isolated yields; the conversions are given in brackets.

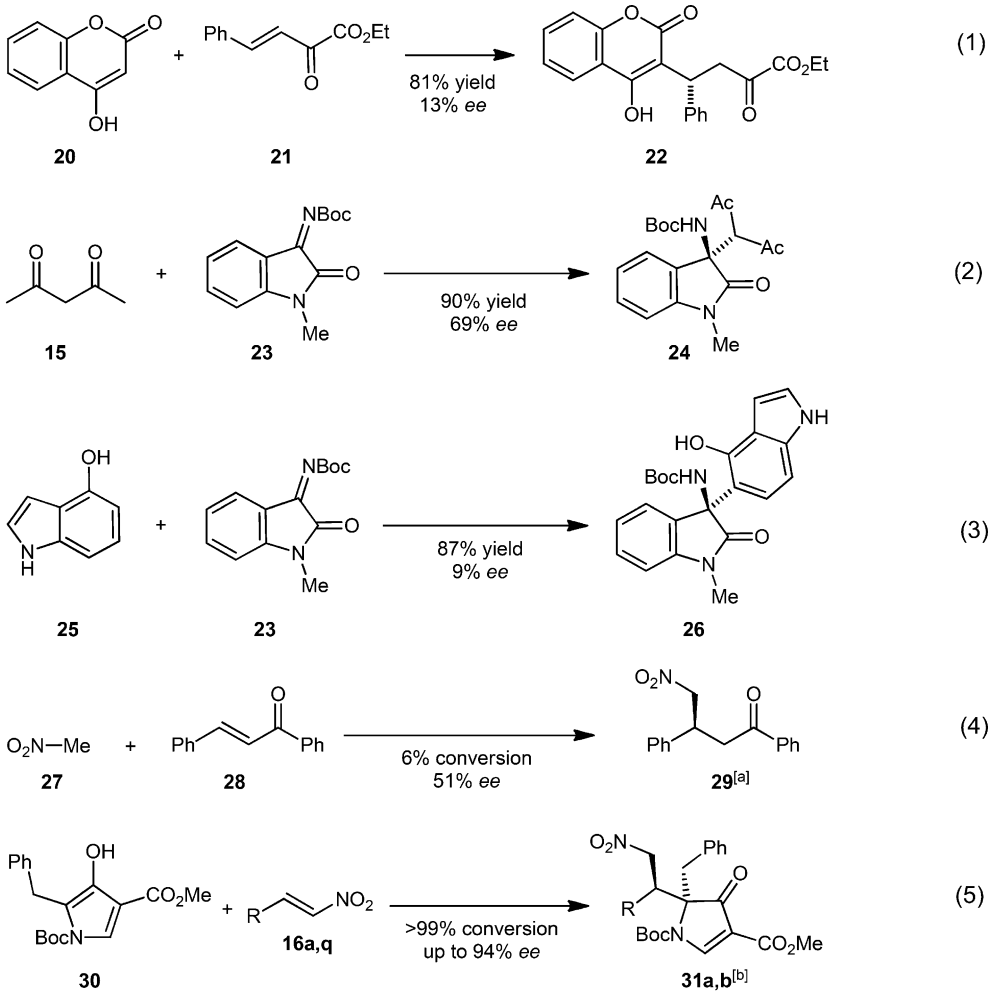

[a] Not isolated.
[b] Tentative configuration.
[c] The *ee* value of the major diastereomer.[21]

Scheme 3. Application of catalyst **9** in some other organic reactions.

trostyrene **16a** (entries 3, 6, and 10 *vs.* 4, 7, 8, 11, and 12).

To quickly explore the scope and limitations in organic synthesis, squaramide **9** was used as catalyst in five other reactions. Notably, only preliminary reactions were preformed devoid of optimization of the reaction conditions. The results are presented in Scheme 3. Promising results (>50% yield, >50% *ee*) were obtained in the 1,2-addition of **15** to isatin imine **23**, and C-alkylation of 3-hydroxypyrrole **30** [Eqs. (2) and (5)]. On the other hand, Michael addition of 4-hydroxycoumarin (**20**) to enone **21** and Friedel–Crafts aminoalkylation of 4-hydroxyindole (**25**) with **23** were not enantioselective, whereas 1,4-addition of nitromethane (**27**) to chalcone (**28**) was enantioselective albeit with low conversion [Eqs. (1), (3), and (4)].[21]

The kinetic profiles of the model reaction, addition of acetylacetone (**15**) to *trans*-β-nitrostyrene (**16a**) in the presence of catalyst **9**, were determined by ^{1}H NMR using different concentrations of the catalyst **9** and reactants **15** and **16a**. Reactions were performed in a rotating NMR tube in 0.75 mL of $CDCl_3$ at 302 K. The results are shown in Figure 3. First, the reaction was carried out under standard conditions (st) using 2.67 mol% catalyst loading and two-fold excess acetylacetone (**15**) ($[\mathbf{9}]_{st} = 1.8 \times 10^{-3}$ M, $[\mathbf{15}]_{st} = 0.14$ M, and $[\mathbf{16a}]_{st} = 0.07$ M) (●). The reversed stoichiometry of reactants using a two-fold excess of β-nitrostyrene (**16a**) (■) did not affect the reaction rate as evidenced by almost identical kinetic profiles (●, ■). With standard concentrations of reactants, $[\mathbf{15}]_{st}$ and $[\mathbf{16a}]_{st}$, and by lowering the catalyst loading to 1.35 mol% (▲) and

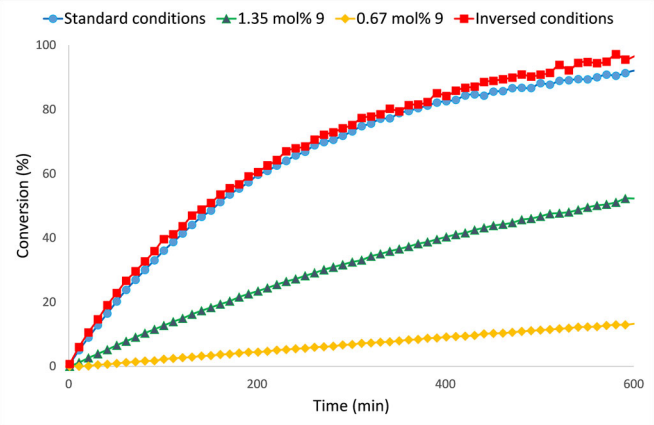

Figure 3. Kinetic profiles of the reaction **15**+**16a**→**17a** in $CDCl_3$ catalyzed with **9**. Standard conditions: $[\mathbf{15}]_{st}=0.14$ M, $[\mathbf{16a}]_{st}=0.07$ M, and $[\mathbf{9}]_{st}=1.8\times10^{-3}$ M (●). Inversed conditions: $[\mathbf{16a}]=0.14$ M, $[\mathbf{15}]=0.07$, $[\mathbf{9}]_{st}$ (■). 1.35 mol% **9**: $[\mathbf{9}]=9\times10^{-4}$ M, $[\mathbf{15}]_{st}$, $[\mathbf{16a}]_{st}$ (▲). 0.67 mol% **9**: $[\mathbf{9}]=4.5\times10^{-4}$ M, $[\mathbf{15}]_{st}$, $[\mathbf{16a}]_{st}$ (◆). The relative conversion of **16a** was determined by integrating the vinylic signal at 7.54 ppm (*d*, $J=$ 13.7 Hz) and by integrating the signal of the product **17a** at 3.88 ppm (*d*, $J=10.0$ Hz).[21]

0.67 mol% (◆), the reaction became much slower (●, ▲, ◆).[21]

Next, the dependences of the initial reaction rates (v_0) of the model reaction on the concentrations of the catalyst and the reactants, [**9**], [**15**], and [**16a**] were determined by ^{1}H NMR by monitoring formation of the product **17a**. The logarithmic initial reaction rates ($\ln v_0$) were plotted against logarithmic concentrations ($\ln c$) as shown in Figure 4 (Plots A–C).[21] When catalyst loading was varied at standard concentrations of the reactants, $[\mathbf{15}]_{st}=0.14$ M and $[\mathbf{16a}]_{st}=$ 0.07 M, a nice linearity between $\ln v_0$ and $\ln$ [**9**] was obtained and the reaction rate showed first-order dependence in the concentration of catalyst **9** (Figure 4, Plot A). Using standard concentrations of the catalyst and the electrophile, $[\mathbf{9}]_{st}=1.8\times10^{-3}$ M and $[\mathbf{16a}]_{st}$, the 0.5-order dependence on the nucleophile **15** was determined in the concentration range $[\mathbf{15}]=0.07$–0.26 M, where the reaction has non-saturation kinetics (Figure 4, Plot B). Kinetic measurements with variable concentrations of the electrophile $[\mathbf{16a}]=0.017$–0.14 M and with standard concentrations $[\mathbf{9}]_{st}$ and $[\mathbf{15}]_{st}$ revealed the first-order dependence of the initial rate on the concentration of **16a** (Figure 4, Plot C).[21] These order dependences were in line with the recently published results on the kinetics of bifunctional squaramide-catalyzed reactions, hence, the reaction most probably follows a bifunctional mechanism with involvement of the ternary complex in the C–C bond formation as the rate-determining step.[23]

Finally, the catalytic retro-Michael reaction on the racemic product ***rac*-17a** was also tested. The measurements were performed in a rotating NMR tube in $CDCl_3$ at 302 K. The concentrations of ***rac*-17a** and **9** were the same ([***rac*-17a**]=[**9**]=0.018 M). The racemic product ***rac*-17a** underwent the reversible process affording acetylacetone (**15**) and *trans*-β-nitrostyrene (**16a**) in 8% conversion within 15 h. Consequently, the remaining Michael adduct **17a** present in the reaction mixture was enantiomerically enriched (7% *ee*) towards the (*R*)-enantiomer meaning that the (*S*)-enantiomer was selectively subjected to the retro-Michael process. According to the principle of microscopic reversibility, these observations indicate that the stereodetermining transition states for forward and backward reaction are the same.[24]

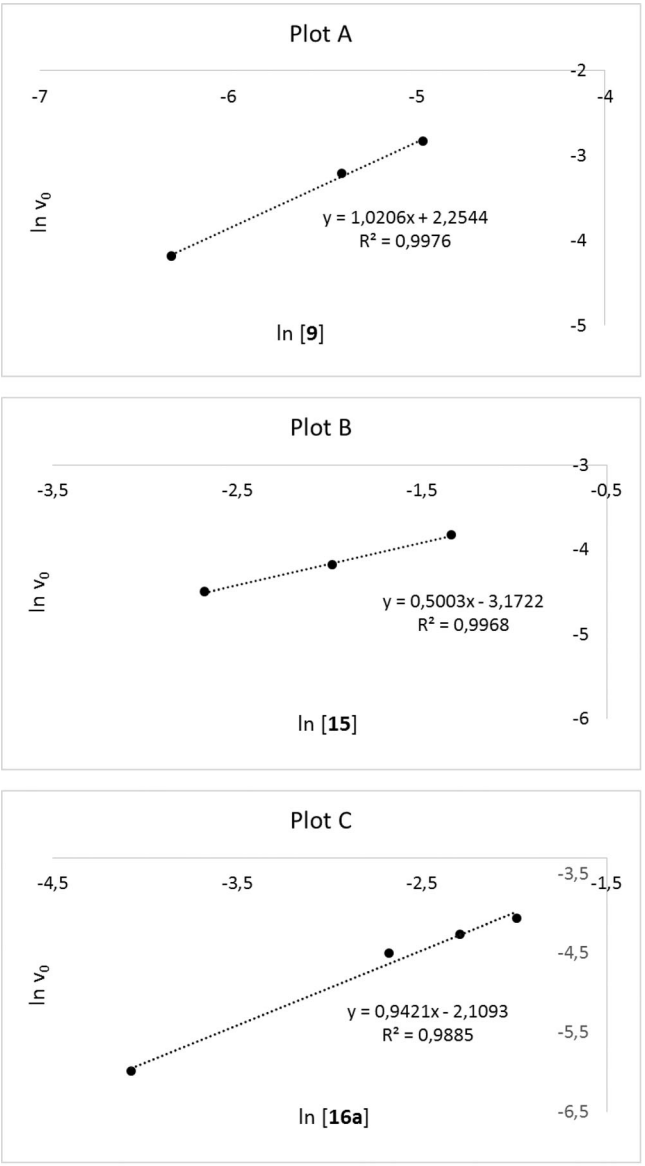

Figure 4. Logarithmic plots of initial reaction rates ($\ln v_0$) against concentration ($\ln c$) of the catalyst **9** (Plot A), acetylacetone (**15**) (Plot B), and nitrostyrene (**16a**) (Plot C).[21]

To gain further insight into the mechanistic aspects and plausible origin of the high enantioselectivity of the 1,3-diamine-derived organocatalyst **9**, density functional theory (DFT) calculations were performed to find the most favored transition state and to compare the results with our experimental data.[21] DFT calculations were carried out for the catalyst **9** and substrates **15** and **16a** leading to the product **17a**, taking into the account that both reactants can form H-bonds with the squaramide unit of the catalyst **9**.[25] Accordingly, all possible orientations leading to the (*R*)- and the (*S*)-isomer were considered and investigated.[21] Figure 5 shows the four transition state structures, **(*S*)-TS1**, **(*R*)-TS1**, **(*S*)-TS2**, and **(*R*)-TS2** that were allocated during the extensive computational scan of the conformational space available to these transition states.

The first pair of transition state structures, **(*S*)-TS1** and **(*R*)-TS1**, corresponds to the Takemoto model:[10b] nitrostyrene **16a** is docked *via* H-bonds to the squaramide unit of the catalyst **9**, whereas the enolate form of the nucleophile **15** is H-bonded to the protonated pyrrolidine part of the catalyst **9**. The second pair of transition state structures, **(*S*)-TS2** and **(*R*)-TS2**, follows the Pápai–Soós model[26] with enolate **15** H-bonded to the squaramide unit of **9** and nitrostyrene (**16a**) H-bonded to the protonated pyrrolidine residue of the catalyst **9**. Within the four proposed transition states, the **(*S*)-TS1** is energetically most favorable. This might be explained by the almost staggered alignment of reactants and a short distance (~0.3 nm) between the pyrrolidine's $H–N^+$ and the oxygen atom of the nitro group both stabilizing **(*S*)-TS1** by dipole-dipole interactions (Figure 5).[21] Formation of the (*S*)-isomer of **17a** *via* energetically most favorable transition state **(*S*)-TS1** suggests that the reaction proceeds through **TS1** following Takemoto's pathway.[10b] This is somewhat surprising, since the alternative Pápai–Soós pathway[26] through **TS2** seems to be dominant for 1,2-diamino catalysis.[25,26] The most favorable transition state **(*S*)-TS1** deriving the (*S*)-isomer of **17a** is in complete agreement with the experimental observations. The corresponding transition state **(*R*)-TS1** leading to the (*R*)-isomer is 3.97 kcal mol^{-1} higher in energy that corresponds to >99% *ee* of the (*S*)-isomer selectivity. Transition states **(*S*)-TS2** and **(*R*)-TS2** are 7.86 and 3.78 kcal mol^{-1} higher in energy, respectively.[21] The observed theoretical data are in line with the results reported by Pápai and Soós et al.[25,26] on a similar catalytic system and support an idea that application of a single reactivity model might not be generalized sufficiently for the realization of the stereoselectivity outcome of Michael additions catalyzed by squaramide-derived organocatalysts.

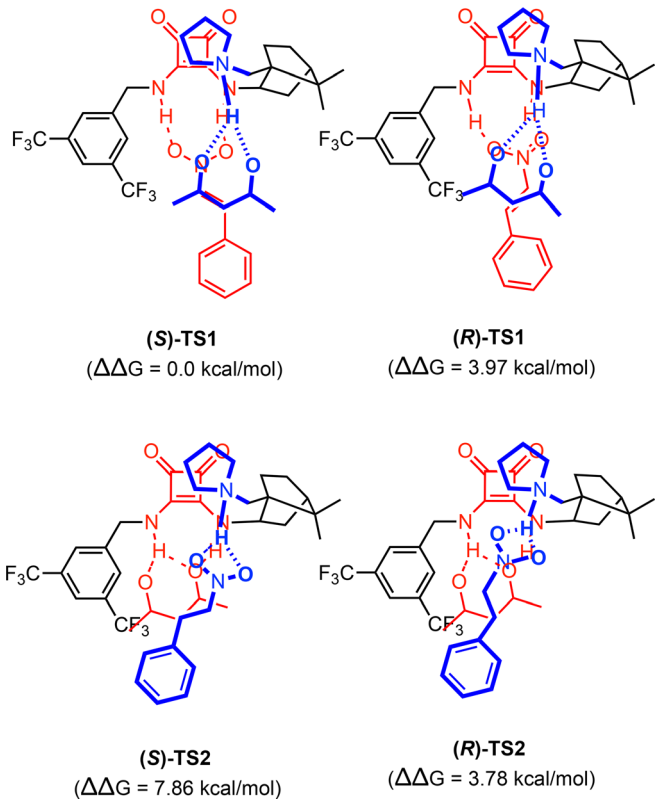

Figure 5. Diagram presentations of the structures of the optimized transition states **(*S*)-TS1**, **(*R*)-TS1**, **(*S*)-TS2**, and **(*R*)-TS2** for the reaction **15**+**16a**→**17a** in the presence of the catalyst **9**. The ΔΔG values are given for the reaction in toluene.

Conclusions

A new class of chiral squaramide catalysts based on a camphor-derived 1,3-diamine scaffold was developed. Organocatalysts **8**–**12** are easily available from (1*S*)-(+)-10-camphorsulfonic acid. Catalyst **9** shows excellent conversions and enantioselectivities (up to >99%) in 1,4-additions of 1,3-dicarbonyls to *trans*-β-nitrostyrene acceptors. It is distinguished by its tolerance towards moisture and air. The kinetic measurements were in agreement with known results on the kinetics of the bifunctional squaramide-catalyzed reactions, thus supporting a bifunctional reaction mechanism.[23] DFT calculations performed on the M06-2X/6-311++G(d,p) level of theory fully corroborate the experimentally observed (*S*)-stereoselectivity of the catalyst **9**. The DFT calculation also suggests that the reaction goes by the Takemoto pathway[10b] through **(*S*)-TS1**. Accordingly, this is the very first time when the original mechanistic proposal seems to be working. The preliminary testing of catalyst **9** in some other reactions also showed promising activities, thus indicating the potential of this class of 1,3-diamine building blocks for the development of new (organo)catalysts. The synthetic method allows for

easy diversification of the core scaffold by attachment of different primary and tertiary amino residues at positions 10 and 2 with *endo*- and *exo*-configuration. Studies on optimization of the synthesis, preparation of novel camphor-1,3-diamine based organocatalysts, and their application in different asymmetric transformations, i.e., **30**→**31** are underway and will be reported it a subsequent communication.

Experimental Section

General

Solvents for extractions and chromatography were of technical grade and were distilled prior to use. Extracts were dried over technical grade Na_2SO_4. Melting points were determined on a Köfler micro hot stage and on SRS OptiMelt MPA100 – Automated Melting Point System (Stanford Research Systems, Sunnyvale, California, USA). The NMR spectra were obtained on a Bruker Avance DPX 300 at 300 MHz for ^{1}H and 75.5 MHz for ^{13}C nucleus, and on a Bruker UltraShield 500 plus (Bruker, Billerica, Massachusetts, USA) at 500 MHz for ^{1}H and 126 MHz for ^{13}C nucleus, using DMSO-d_6 and $CDCl_3$ with TMS as the internal standard, as solvents. Mass spectra were recorded on an Agilent 6224 Accurate Mass TOF LC/MS (Agilent Technologies, Santa Clara, California, USA), IR spectra on a Perkin–Elmer Spectrum BX FTIR spectrophotometer (Perkin–Elmer, Waltham, Massachusetts, USA). Microanalyses were performed on a Perkin–Elmer CHN Analyzer 2400 II (PerkinElmer, Waltham, Massachusetts, USA). Column chromatography (CC) was performed on silica gel [Silica gel 60, particle size: 0.035–0.070 mm (Sigma–Aldrich, St. Louis, Missouri, USA)]. HPLC analyses were performed on an Agilent 1260 Infinity LC (Agilent Technologies, Santa Clara, California, USA) using CHIRALPAK AD-H (0.46 cm ø×25 cm) and CHIRALCEL OD-H (0.46 cm ø× 25 cm) chiral columns (Chiral Technologies, Inc., West Chester, Pennsylvania, USA). Organocatalyzed reactions were performed on EasyMax 102 Advanced synthesis workstation (Mettler-Toledo, LLC).

All the chemicals used are commercially available and were purchased from Sigma–Aldrich (St. Louis, Missouri, USA). The source of chirality: (1*S*)-(+)-10-camphorsulfonic acid (**1**), product number C2107 Aldrich, assay: ≥99.0%, $[\alpha]_D^{20}$: +19.9° (*c*=5 in H_2O), mp 196–200 °C (dec.).

Synthesis of Organocatalyst 9

To a solution of *endo*-1,3-diamine **5** (4.542 mmol, 1.01 g) in anhydrous MeOH (25 mL) under argon squaramide **6a** (4.954 mmol, 1.75 g) was added and the reaction mixture was stirred at room temperature for 48 h. The resulting precipitate was collected by filtration and washed with cooled Et_2O (0 °C, 2×20 mL) to give product **9** as a white solid; yield: 2.068 g (3.805 mmol, 84%); mp 226–229 °C. $[\alpha]_D^{r.t.}$: −37.9 (*c*=0.34, CH_2Cl_2:MeOH=1:1). Anal.: $C_{27}H_{31}F_6N_3O_2$ requires: C 59.66, H 5.75, N 7.73; found: C 59.74, H 5.52, N 7.68%; EI-HR-MS: *m/z*=544.2393 (MH^+); $C_{27}H_{32}F_6N_3O_2$ requires: 544.2393 (MH^+); IR: ν_{max}=3306, 3215, 2956, 2875, 2800, 1801, 1657, 1539, 1489, 1457, 1417, 1381, 1343, 1301, 1276, 1170, 1129, 1001, 952, 896, 871, 843, 822, 731, 722, 707, 681, 617 cm^{-1}. ^{1}H NMR (500 MHz, DMSO-d_6): δ=0.85 (*s*, 3H, Me), 0.90 (*s*, 3H, Me), 0.87–0.99 (*m*, 1H), 1.08–1.32 (*m*, 5H), 1.37–1.48 (*m*, 1H), 1.57 (*t*, *J*=4.4 Hz, 1H), 1.73–1.83 (*m*, 1H), 1.85–1.95 (*m*, 1H), 2.00 (*d*, *J*=12.6 Hz, 1H), 2.05–2.15 (*m*, 2H), 2.18–2.28 (*m*, 2H), 2.28–2.39 (*m*, 1H), 2.73 (*d*, *J*=12.5 Hz, 1H), 4.57–4.67 (*m*, 1H), 4.84 (*dd*, *J*=15.3, 5.8 Hz, 1H), 4.93 (*dd*, *J*=15.0, 7.2 Hz, 1H), 7.41 (*d*, *J*=10.2 Hz, 1H, NH), 7.58 (*s*, 1H, NH), 8.06 (*s*, 1H, 1H of Arl), 8.11 (*s*, 2H, 2H of Arl); ^{13}C NMR (126 MHz, DMSO-d_6): δ=18.8, 20.1, 23.0, 25.4, 28.4, 37.5, 44.0, 45.5, 48.9, 51.9, 54.9, 57.0, 57.4, 121.2, 123.3 (*q*, *J*=272.8 Hz), 128.8 (*d*, *J*=4.0 Hz), 130.48 (q, *J*=32.7 Hz), 143.0, 165.5, 169.5, 182.3, 182.9.

General Procedure for the Organocatalyzed Asymmetric Michael Addition of 1,3-Dicarbonyl Nucleophiles to Nitroalkene Acceptors

To a solution/suspension of nitroalkene acceptor (0.4 mmol) and the tested organocatalyst **8**–**12** (0.1–5 mmol%) in anhydrous solvent (1 mL) under argon at the designated temperature (*T*=−25 °C to 80 °C) the 1,3-dicarbonyl nucleophile was added (0.8 mmol) and the resulting reaction mixture was stirred for 3–24 h. The reaction was quenched by passing it as quickly as possible through a short pad of silica gel 60 (length 3–4 cm, diameter=2 cm) using a mixture of EtOAc and petroleum ether in a ratio of 1:1 to cut off the organocatalyst used. Volatile components were evaporated under vacuum. The residue was used to determine the reaction conversion and diastereomer ratio by means of ^{1}H NMR analysis and the enantiomer excess of the products by means of HPLC analysis. The novel organocatalyzed products were isolated by column chromatography (silica gel 60, mobile phase). Fractions containing the pure product were combined and volatile components evaporated under vacuum followed by full characterization.

General Procedure for the Preparation of Racemic Mixtures

To a solution/suspension of nitroalkene acceptor (0.4 mmol) and achiral organocatalyst **13** (0.0244 mmol, 10 mg) in CH_2Cl_2 (2 mL) at room temperature the 1,3-dicarbonyl compound was added (0.8 mmol) and the resulting reaction mixture was stirred at room temperature for 24 h. Volatile components were evaporated under vacuum and the residue was purified by column chromatography (Silica gel 60, mobile phase). Fractions containing the pure racemic product(s) were combined and volatile components evaporated under vacuum followed by HPLC analysis.

Acknowledgements

Financial support from the Slovenian Research Agency through grant P1-0179 is gratefully acknowledged.

References

[1] a) J. Seayad, B. List, *Org. Biomol. Chem.* **2005**, *3*, 719–724; b) P. I. Dalko, L. Moisan, *Angew. Chem.* **2004**, *116*, 5248–5286; *Angew. Chem. Int. Ed.* **2004**, *43*, 5138–5175; c) K. N. Houk, B. List, *Acc. Chem. Res.* **2004**, *37*, 487–487.

[2] a) *Stereoselective Organocatalysis*, (Ed.: R. Rios), John Wiley & Sons, Hoboken, **2013**; b) G. Jakab, P. R. Schreiner, in: *Comprehensive Enantioselective Organocatalysis*, (Ed.: P. I. Dalko), Wiley-VCH, Weinheim, **2013**, pp 315–342.

[3] For recent reviews on bifunctional amine-thioureas, see: a) M. S. Taylor, E. N. Jacobsen, *Angew. Chem.* **2006**, *118*, 1550–1573; *Angew. Chem. Int. Ed.* **2006**, *45*, 1520–1543; b) Z. Zhang, P. R. Schreiner, *Chem. Soc. Rev.* **2009**, *38*, 1187–1198; c) S. J. Connon, *Synlett* **2009**, 354–376; d) W.-Y. Siau, J. Wang, *Catal. Sci. Technol.* **2011**, *1*, 1298–1310; e) S. Narayanaperumal, D. G. Rivera, R. C. Silva, M. W. Paixao, *ChemCatChem* **2013**, *5*, 2756–2773; f) O. V. Serdyuk, C. M. Heckel, S. B. Tsogoeva, *Org. Biomol. Chem.* **2013**, *11*, 7051–7071.

[4] For recent reviews on bifunctional amine-squaramides, see: a) F. E. Held, S. B. Tsogoeva, *Catal. Sci. Technol.* **2016**, *6*, 645–667; b) P. Chauhan, S. Mahajan, U. Kaya, D. Hack, D. Enders, *Adv. Synth. Catal.* **2015**, *357*, 253–281; c) J. Alemán, A. Parra, H. Jiang, K. A. Jørgensen, *Chem. Eur. J.* **2011**, *17*, 6890–6899. For examples of squaramide-derived organocatalysts. see: d) Y. Zhu, J. P. Malerich, V. H. Rawal, *Angew. Chem.* **2010**, *122*, 157–160; *Angew. Chem. Int. Ed.* **2010**, *49*, 153–156; e) J. P. Malerich, K. Hagihara, V. H. Rawal, *J. Am. Chem. Soc.* **2008**, *130*, 14416–14417.

[5] For selected examples of construction of multiple stereogenic centers by organocatlysis see: a) P. Chauhan, S. Mahajan, C. C. J. Loh, G. Raabe, D. Enders, *Org. Lett.* **2014**, *16*, 2954–2957; b) M. Bluemel, P. Chauhan, R. Hahn, G. Raabe, D. Enders, *Org. Lett.* **2014**, *16*, 6012–6015; c) C. C. J. Loh, P. Chauhan, D. Hack, C. Lehmann, D. Enders, *Adv. Synth. Catal.* **2014**, *356*, 3181–3186; d) P. Chauhan, G. Urbanietz, G. Raabe, D. Enders, *Chem. Commun.* **2014**, *50*, 6853–6855; e) P. Chauhan, S. Mahajan, G. Raabe, D. Enders, *Chem. Commun.* **2015**, *51*, 2270–2272; f) D. Mailhol, M. del Mar Sanchez Duque, W. Raimondi, D. Bonne, T. Constantieux, Y. Coquerel, J. Rodriguez, *Adv. Synth. Catal.* **2012**, *354*, 3523–3532.

[6] D. Steinborn, *Fundamentals of Organometallic Catalysis*, Wiley-VCH, Weinheim, **2016**.

[7] a) Y. L. Bennani, S. Hanessian, *Chem. Rev.* **1997**, *97*, 3161–3195; b) R. Noyori, T. Ohkuma, *Angew. Chem.* **2001**, *113*, 40–75; *Angew. Chem. Int. Ed.* **2001**, *40*, 40–73; c) W. Notz, F. Tanaka, C. F. Barbas III, *Acc. Chem. Res.* **2004**, *37*, 580–591; d) J. Duan, P. Li, *Catal. Sci. Technol.* **2014**, *4*, 311–320.

[8] M. S. Sigman, E. N. Jacobsen, *J. Am. Chem. Soc.* **1998**, *120*, 4901–4902.

[9] P. R. Schreiner, A. Wittkopp, *Org. Lett.* **2002**, *4*, 217–220.

[10] a) T. Okino, Y. Hoashi, Y. Takemoto, *J. Am. Chem. Soc.* **2003**, *125*, 12672–12673; b) T. Okino, Y. Hoashi, T. Furukawa, X. Xu, Y. Takemoto, *J. Am. Chem. Soc.* **2005**, *127*, 119–125; c) H. Miyabe, Y. Takemoto, *Bull. Chem. Soc. Jpn.* **2008**, *81*, 785–795; d) Y. Takemoto, *Chem. Pharm. Bull.* **2010**, *58*, 593–601.

[11] a) P. Melchiorre, *Angew. Chem.* **2012**, *124*, 9886–9909; *Angew. Chem. Int. Ed.* **2012**, *51*, 9748–9770; b) L. Zhang, N. Fu, S. Luo, *Acc. Chem. Res.* **2015**, *48*, 986–997.

[12] a) Y. Sohtome, B. Shin, N. Horitsugi, R. Takagi, K. Noguchi, K. Nagasawa, *Angew. Chem.* **2010**, *122*, 7457–7461; *Angew. Chem. Int. Ed.* **2010**, *49*, 7299–7303; b) Y. Sohtome, N. Horitsugi, R. Takagi, K. Nagasawa, *Adv. Synth. Catal.* **2011**, *353*, 2631–2636; c) W. Yao, M. Chen, X. Liu, R. Jiang, S. Zhang, W. Chen, *Catal. Sci. Technol.* **2014**, *4*, 1726–1729; d) X. Ren, C. He, Y. Feng, Y. Chai, W. Yao, W. Chen, S. Zhang, *Org. Biomol. Chem.* **2015**, *13*, 5054–5060; e) W.-H. Wang, T. Abe, X.-B. Wang, K. Kodama, T. Hirose, G.-Y. Zhang, *Tetrahedron: Asymmetry* **2010**, *21*, 2925–2933; f) M. B. Lauber, R. Fröhlich, J. Paradies, *Synthesis* **2012**, *44*, 3209–3215.

[13] a) T. Money, *Remote functionalization of camphor: application to natural product synthesis*, in: *Org. Synth.: Theory Appl.* **1996**, 3, 1–83; b) T. Money, *Nat. Prod. Rep.* **1985**, *2*, 253–289.

[14] a) M. Lemay, W. W. Ogilvie, *Org. Lett.* **2005**, *7*, 4141–4144; b) S. Rajaram, M. S. Sigman, *Org. Lett.* **2005**, *7*, 5473–5475.

[15] U. Grošelj, *Curr. Org. Chem.* **2015**, *19*, 2048–2074.

[16] a) Y. Li, Z. Feng, S.-L. You, *Chem. Commun.* **2008**, 2263–2265; b) Q. Li, W.-Y. Wong, W.-H. Chan, A. W. M. Lee, *Adv. Synth. Catal.* **2010**, *352*, 2142–2146; c) Y. Li, X.-Q. Wang, C. Zheng, S.-L. You, *Chem. Commun.* **2009**, 5823–5825; d) Z.-Q. Rong, M.-Q. Jia, S.-L. You, *Org. Lett.* **2011**, *13*, 4080–4083.

[17] For selected examples, see: a) Y.-m. Chen, P.-H. Lee, J. Lin, K. Chen, *Eur. J. Org. Chem.* **2013**, 2699–2707; b) Y. Zhou, Q. Liu, Y. Gong, *Org. Biomol. Chem.* **2012**, *10*, 7618–7627; c) Y.-F. Ting, C. Chang, R. J. Reddy, D. R. Magar, K. Chen, *Chem. Eur. J.* **2010**, *16*, 7030–7038; d) D. R. Magar, C. Chang, Y.-F. Ting, K. Chen, *Eur. J. Org. Chem.* **2010**, 2062–2066; e) C. Chang, S.-H. Li, R. J. Reddy, K. Chen, *Adv. Synth. Catal.* **2009**, *351*, 1273–1278.

[18] a) U. Grošelj, A. Golobič, K. Stare, J. Svete, B. Stanovnik, *Chirality* **2012**, *24*, 307–317; b) U. Grošelj, S. Ričko, J. Svete, B. Stanovnik, *Chirality* **2012**, *24*, 412–419; c) S. Ričko, A. Golobič, J. Svete, B. Stanovnik, U. Grošelj, *Chirality* **2015**, *27*, 39–52.

[19] a) J. D. Loudon, *J. Chem. Soc.* **1933**, 823–825; b) F. W. Lewis, G. Egron, D. H. Grayson, *Tetrahedron: Asymmetry* **2009**, *20*, 1531–1535; c) M. J. Spallek, G. Storch, O. Trapp, *Eur. J. Org. Chem.* **2012**, 3929–3945.

[20] a) K. S. Rao, R. Trivedi, M. L. Kantam, *Synlett* **2015**, *26*, 221–227; b) Y. Qian, G. Ma, A. Lv, H.-L. Zhu, J. Zhao, V. H. Rawal, *Chem. Commun.* **2010**, *46*, 3004–3006.

[21] For details see the Supporting Information.

[22] Structural and other crystallographic data have been deposited. CCDC 1476085 and CCDC 1476086 contain the supplementary crystallographic data for compounds **9** and **10**, respectively, of this paper. These data can be obtained free of charge from The Cambridge Crystallo-

graphic Data Centre *via* www.ccdc.cam.ac.uk/data_request/cif.
[23] E. Varga, L. T. Mika, A. Csámpai, T. Holczbauer, G. Kardos, T. Soós, *RSC Adv.* **2015**, *5*, 95079–95086.
[24] D. G. Blackmond, O. K. Matar, *J. Phys. Chem. B* **2008**, *112*, 5098–5104.
[25] B. Kótai, G. Kardos, A. Hamza, V. Farkas, I. Pápai, T. Soós, *Chem. Eur. J.* **2014**, *20*, 5631–5639.
[26] a) A. Hamza, G. Schubert, T. Soós, I. Pápai, *J. Am. Chem. Soc.* **2006**, *128*, 13151–13160; b) B. Tan, Y. Lu, X. Zeng, P. J. Chua, G. Zhong, *Org. Lett.* **2010**, *12*, 2682–2685.